


# Quadrupole phonon excitations and transition probabilities for low-lying states of neutron-rich Cd isotopes

Y. Bao, Y. Y. Cheng <sup>\*</sup>, and Xian-Rong Zhou *Department of Physics, East China Normal University, Shanghai 200241, China* (Received 5 March 2021; revised 1 May 2021; accepted 11 August 2021; published 14 September 2021)

In this paper we study the low-lying states of neutron-rich  $^{122,124,126,128}\text{Cd}$  and  $^{130,132,134,136,138}\text{Cd}$  within the nucleon-pair approximation of the shell model. We adopt the phenomenological Hamiltonian for  $^{122,124,126,128}\text{Cd}$ , and the shell-model effective interaction  $jj46$  for  $^{130,132,134,136,138}\text{Cd}$ . The available experimental excitation energies and quadrupole transition probabilities are well reproduced by our calculation, and we also make predictions for very neutron-rich Cd nuclei. Based on our calculation, the  $B(E2; 0_{\text{g.s.}}^+ \rightarrow 2_1^+)$  values exhibit an asymmetric feature with respect to the  $N = 82$  shell closure, which mainly comes from the contributions of the proton transition matrix elements. We also investigate for the eight open-shell Cd nuclei, whether two low-lying yrast states with spins differing by 2 can be connected by a quadrupole-phonon excitation, and here we take the proton and neutron quadrupole operators multiplied by  $1/r_0^2$  as our quadrupole phonon operators. We calculate explicit overlaps between the low-lying yrast states and the constructed quadrupole-phonon states based on the low-lying yrast states with lower spins, and the results indicate that, for all eight open-shell Cd nuclei,  $|2_1^+\rangle$  and  $|4_1^+\rangle$  can be well described to be the states constructed by coupling the proton or neutron phonon to  $|0_{\text{g.s.}}^+\rangle$  and  $|2_1^+\rangle$ , respectively. Very interestingly, for  $^{126,124,122}\text{Cd}$  and  $^{136,138}\text{Cd}$ , the  $2_1^+$  state can be well described to be both the proton phonon state and the neutron phonon state, which indicates a nonorthogonal feature of these two phonon states. We further present an analytic relation for the overlap between these two phonon states, which implies that the proton and neutron phonon states constructed using the quadrupole operators and the  $0_{\text{g.s.}}^+$  state in an open-shell nucleus are almost impossibly orthogonal.

DOI: [10.1103/PhysRevC.104.034312](https://doi.org/10.1103/PhysRevC.104.034312)

## I. INTRODUCTION

Cd isotopes (with  $Z = 48$ ) are of particular interest in nuclear physics. The very long chain from  $^{96}\text{Cd}$  to  $^{132}\text{Cd}$ , with experimental information for low-lying states, provides a very good case for studies regarding nuclear structure changes associated with the change of the isospin, as well as changes associated with the crossing of the  $N = 50$  shell closure, the gradual filling of the  $N = 50 - 82$  major shell, and the crossing of the  $N = 82$  shell closure. The low-lying states of Cd isotopes also manifest themselves as good examples of vibrational states, which are interpreted to be surface oscillations of a liquid drop with respect to the equilibrium shape in the macroscopic view [1]. Nuclei around  $^{100}\text{Sn}$  and  $^{132}\text{Sn}$  are also of importance to astrophysical studies of the  $rp$  process and  $r$  process.

In Refs. [2–4], the  $E(2_1^+)$  and  $B(E2; 0_{\text{g.s.}}^+ \rightarrow 2_1^+)$  for Cd isotopes have been systematically studied, based on the Skyrme and Gogny energy density functionals (EDFs), respectively. In Ref. [2], these observables for the long chain spanning the  $N = 50-82$  major shell were studied using the beyond-mean-field approach with the Gogny force. In Ref. [3], those for the Cd nuclei from  $N = 62$  to 84 were studied using the generator coordinate method (GCM) with various Skyrme forces and pairing forces. In Ref. [4], those

for the Cd nuclei from  $N = 78$  to 86 were studied using the quasiparticle random phase approximation (QPRA) including the phonon-phonon coupling (PPC) together with the Skyrme interaction.

Within the interacting boson model (IBM) [5], low-lying states of Cd isotopes with  $A = 110 - 116$  have been intensively studied; see, e.g., Refs. [6–12]. The important role played by the interplay between the normal spherical-vibrator states with the  $U(5)$  symmetry and the intruder states characterized by the  $I$ -spin quantum number was emphasized for the low-lying yrast and side bands of  $^{110,112,114}\text{Cd}$  in Refs. [6,7]; but with more available experimental data of  $^{112,114,116}\text{Cd}$ , it was debated [8–11]. Instead, a recent study [12] where the  $U(5)$  partial dynamical symmetry was considered, i.e., particular phonon states were mixed, provided a very good description to the low-lying yrast and nonyrast states of  $^{110}\text{Cd}$ .

For the most neutron-deficient  $^{96}\text{Cd}$  with  $N = Z = 48$ , low-lying yrast states are intensively discussed in terms of spin-aligned isoscalar proton-neutron pairs within the shell model and in terms of  $b$  bosons within the IBM; see, e.g., Refs. [13–18].

For the neutron-rich Cd nuclei, within the shell model (SM), the low-lying states are described to be the states of a few valence neutron holes or particles together with two valence proton holes coupled to the  $^{132}\text{Sn}$  core. Such a picture relies on the persistence of the  $Z = 50$  and  $N = 82$  shell gaps. An earlier experimental result of  $^{130}\text{Cd}$  indicated a quenching of the  $N = 82$  shell [19], while recent results regarding the

\*Corresponding author: [yycheng@phy.ecnu.edu.cn](mailto:yycheng@phy.ecnu.edu.cn)

isomeric decays in  $^{130}\text{Cd}$  and in  $^{128,126}\text{Pd}$  gave evidence of a robust  $N = 82$  shell closure in neutron-rich Cd and Pd nuclei [20,21]. In Ref. [22], the shell-model description of  $B(E2; 0_{\text{g.s.}}^+ \rightarrow 2_1^+)$  of  $^{124,126}\text{Cd}$  was shown to agree well with the experimental data. In Ref. [23], a shell-model effective interaction for the southeast region with respect to the  $^{132}\text{Sn}$  nucleus was presented, with the calculated excitation energies of low-lying states of  $^{130}\text{Cd}$  reproducing experimental data very well.

In this work we study neutron-rich  $^{122,124,126,128}\text{Cd}$  and  $^{130,132,134,136,138}\text{Cd}$  nuclei within the nucleon-pair approximation (NPA) [24,25], which is a pair-truncation scheme of the nuclear shell model based on the technique of calculating the commutators between coupled fermion clusters [26]. Such a pair-truncation scheme of the shell model is shown to be able to give a good description of low-lying states of semimagic nuclei, transitional nuclei, and well-deformed nuclei; see, e.g., Refs. [27–38]. In Refs. [35,36] it was shown that for low-lying states of the discussed semimagic nuclei the SM wave function can be well approximated as one optimized nucleon-pair basis state, i.e., the SM wave function is approximately one-dimensional in terms of coupled pair basis states; and in Ref. [39] for nucleons in single- $j$  shells, very compact analytic expressions for wave functions of eigenstates with respect to any two-body interactions were given in terms of coupled pair basis states. The NPA with isospin symmetry [40], the version with particle-hole excitations [41], and the versions considering pairs in the  $M$  scheme [42,43] have been developed in recent years. For a comprehensive review, see Ref. [44].

For  $^{130,132,134,136,138}\text{Cd}$ , we adopt the  $jj46$  effective interaction of Ref. [23], where the proton-proton and neutron-neutron parts are both renormalized from the realistic CD-Bonn potential [45] using the  $G$ -matrix method [46], and the proton-neutron part is derived from the monopole-based universal interaction  $V_{MU}$  [47] plus the M3Y spin-orbit force [48]. It was shown in Ref. [23] that the  $jj46$  SM effective interaction provides a good description for low-lying states of nuclei near  $^{132}\text{Sn}$  in this region. For Cd nuclei with  $N \geq 82$ , their low-lying states are close to the limit of current experimental access, thus experimental data are sparse. In this work, using the NPA together with the  $jj46$  interaction, our results agree well with available experimental results for  $^{130}\text{Cd}$  [20] and  $^{132}\text{Cd}$  [49], and we further make predictions for excitation energies and  $B(E2)$  values for low-lying states of these Cd nuclei up to  $^{138}\text{Cd}$ .

For  $^{128,126,124,122}\text{Cd}$ , we adopt the phenomenological Hamiltonian including monopole pairing, quadrupole pairing, quadrupole-quadrupole interactions, as well as the proton-hole highest-spin pairing interaction with spin 8 and the neutron-hole highest-spin pairing interaction with spin 10. A set of strength parameters are obtained by adjusting to fit the experimental data of these four nuclei. Our NPA results with such a shell-model Hamiltonian reproduce experimental energy levels and available  $B(E2)$  values very well.

The low-lying yrast excited states of the Cd nuclei discussed here are expected to be collective vibrational states with respect to the spherical equilibrium. The (Q)RPA [50,51] and the IBM [5] are successful in describing such states

microscopically. In the (Q)RPA [50,51] the low-lying excited states are regarded to be the one-phonon excited states with respect to the (Q)RPA ground state, and by solving the (Q)RPA equations the structure of the phonon, as well as the structure of corresponding collective vibration, is determined. Within the IBM [5], in the  $U(5)$  limit the  $d$  boson maps to the quadrupole phonon in the harmonic quadrupole vibration of a spherical liquid drop [52], thus the quanta of the  $d$  boson number characterize the quadrupole vibrational states with respect to the spherical equilibrium. In Refs. [53–55] interesting generalizations to non- $U(5)$  cases with  $\beta$  and  $\gamma$  vibrations, by introducing two different types of  $d$  bosons, are discussed.

From another perspective, based on the NPA wave functions obtained by diagonalization in the pair-truncated shell-model spaces, we investigate in this work whether two low-lying yrast states with spins differing by 2 can be connected by a quadrupole-phonon excitation, for  $^{128,126,124,122}\text{Cd}$  and  $^{132,134,136,138}\text{Cd}$ . We couple the quadrupole phonon defined below to the low-lying yrast states with spin  $(I - 2)$  to construct phonon states with spin  $I$ , and calculate explicit overlaps between the phonon states and the low-lying yrast states. For the phonon operators, we consider here components of a dimensionless spherical tensor of rank 2, which are the proton or neutron quadrupole operators, i.e.,

$$Q^{(2)}(\tau) = \sum_{k \in \{\tau\}} r_k^2 Y^{(2)}(\theta_k, \varphi_k), \quad \tau = \pi \text{ or } \nu, \quad (1)$$

divided by  $r_0^2$  ( $r_0$  is the size parameter of the nucleus, which is taken to be  $r_0 = \sqrt{\frac{\hbar}{m\omega}}$  when using the harmonic-oscillator single-particle wave function within the shell-model framework). Here the subscript  $k$  denotes the  $k$ th valence particle or hole, and  $(r_k, \theta_k, \varphi_k)$  are its spherical coordinates;  $\{\pi\}$  consists of valence proton holes, and  $\{\nu\}$  consists of valence neutron holes for Cd nuclei with  $N < 82$  and of valence neutron particles for Cd nuclei with  $N > 82$ .

In this work we also study the quadrupole transition probabilities  $B(E2; 0_{\text{g.s.}}^+ \rightarrow 2_1^+)$  of the nine Cd nuclei and their evolution with increasing mass number  $A$ , in terms of corresponding proton and neutron transition matrix elements  $M_\pi$  and  $M_\nu$ .

This paper is organized as follows. In Sec. II we briefly introduce our theoretical framework, including the configuration space constructed by coupled nucleon pairs and two shell-model Hamiltonians adopted in this work. In Sec. III we present and discuss our calculated results for these nine Cd nuclei. In Sec. IV we summarize our paper.

## II. THEORETICAL FRAMEWORK

### A. Nucleon-pair configurations

We begin with the definition of nucleon-pair operators. The creation operator of a collective nucleon pair with spin  $r$  is defined by

$$A^{(r)\dagger} \equiv A_\mu^{(r)\dagger} = \sum_{j_1 j_2} y(j_1 j_2 r) A^{(r)\dagger}(j_1 j_2), \quad (2)$$

$$A^{(r)\dagger}(j_1 j_2) \equiv A_\mu^{(r)\dagger}(j_1 j_2) = (a_{j_1}^\dagger \times a_{j_2}^\dagger)_\mu^{(r)},$$

where  $A^{(r)\dagger}(j_1 j_2)$  is a noncollective pair, and  $(a_{j_1}^\dagger \times a_{j_2}^\dagger)_\mu^{(r)} = \sum_{m_1 m_2} C_{j_1 m_1 j_2 m_2}^{r\mu} a_{j_1 m_1}^\dagger a_{j_2 m_2}^\dagger$  with  $C_{j_1 m_1 j_2 m_2}^{r\mu}$  the Clebsch-Gordan coefficient. Here we denote the creation operator of a particle in the orbit associated with quantum numbers  $(n, l, j, m)$  by using  $a_{jm}^\dagger \equiv a_{nljm}^\dagger$ . A collective pair creation operator  $A^{(r)\dagger}$  is given by the linear combination of all noncollective pairs with spin  $r$ , with  $y(j_1 j_2 r)$  the so-called structure coefficient. For a system with  $2N$  identical valence nucleons, the pair basis states are constructed by coupling  $N$  nucleon pairs successively,

$$[(A^{(r_1)\dagger} \times A^{(r_2)\dagger})^{(J_2)} \times \dots \times A^{(r_N)\dagger}]^{(J_N)} |0\rangle. \quad (3)$$

The structure coefficients play a key role in the validity of corresponding pair truncation. Below we briefly introduce how we fix the structure coefficients in this work. We consider first the  $S$  pair with spin 0. We define

$$S^\dagger = \sum_j y(jj0) (a_j^\dagger \times a_j^\dagger)^{(0)} = \sum_j y(jj0) S_j^\dagger. \quad (4)$$

Then for the system with  $2N$  nucleons the structure coefficients  $y(jj0)$  are determined variationally to minimize the energy expectation of the  $S$ -pair-condensate state [56], i.e., determined by solving the following equation

$$\delta \frac{\langle S^N | H | S^N \rangle}{\langle S^N | S^N \rangle} = 0. \quad (5)$$

$$\varepsilon_{j\pi 1} = -e_{j\pi 1} - \frac{1}{2j_{\pi 1} + 1} \sum_{j_\pi} \sum_J (1 + \delta_{j_\pi 1, j_\pi 2}) (2J + 1) \langle j_{\pi 1} j_{\pi 2} J | \hat{v} | j_{\pi 1} j_{\pi 2} J \rangle,$$

$$\varepsilon_{j\nu} = e_{j\nu} + \frac{1}{2j_\nu + 1} \sum_{j_\pi} \sum_J (2J + 1) \langle j_\pi j_\nu J | \hat{v} | j_\pi j_\nu J \rangle,$$

$$V_J^{\pi\pi}(j_{\pi 1} j_{\pi 2} j_{\pi 3} j_{\pi 4}) = \langle j_{\pi 1} j_{\pi 2} J | \hat{v} | j_{\pi 3} j_{\pi 4} J \rangle,$$

$$V_J^{\pi\nu}(j_{\pi 1} j_{\nu 1} j_{\pi 2} j_{\nu 2}) = - \sum_{J'} (2J' + 1) \begin{Bmatrix} j_{\pi 2} & j_{\nu 1} & J' \\ j_{\pi 1} & j_{\nu 2} & J \end{Bmatrix} \langle j_{\pi 2} j_{\nu 1} J' | \hat{v} | j_{\pi 1} j_{\nu 2} J' \rangle. \quad (7)$$

Here  $e_j$  is the single-particle energy with respect to the core of  $Z = 28$  and  $N = 82$ , and  $\langle |\hat{v}| \rangle$  is the normalized two-body matrix element of two valence particles, taken from the  $jj46$  Hamiltonian;  $\varepsilon_{j\pi}$  and  $\varepsilon_{j\nu}$  are the single proton-hole energy and single neutron-particle energy with respect to the core of  $Z = 50$  and  $N = 82$ , and  $V_J^{\pi\pi}(j_{\pi 1} j_{\pi 2} j_{\pi 3} j_{\pi 4})$  and  $V_J^{\pi\nu}(j_{\pi 1} j_{\nu 1} j_{\pi 2} j_{\nu 2})$  are the normalized two-body matrix element of two valence proton holes and the normalized two-body matrix element of a valence proton hole and a valence neutron particle, used in our calculation.

For  $^{128,126,124,122}\text{Cd}$ , we consider valence proton holes in the 28-50 major shell and valence neutron holes in the 50-82 major shell. The following phenomenological Hamiltonian including monopole pairing, quadrupole pairing, and quadrupole-quadrupole interactions is adopted, and the proton-hole highest-spin pairing interaction with spin 8 and the neutron-hole highest-spin pairing interaction with spin 10 are additionally included to give a good description to the  $8_1^+$

We consider next a non- $S$  pair with spin  $r$  ( $r \neq 0$ ). We diagonalize the SM Hamiltonian in the  $(S^\dagger)^{(N-1)} A^{(r)\dagger}(j_1 j_2)$  space with  $j_1, j_2$  running over all the  $j$  orbits, namely in the space with a generalized-seniority number  $\nu = 2$ . The lowest-energy wave function is written in the form

$$(S^\dagger)^{(N-1)} \sum_{j_1 j_2} c(j_1 j_2) A^{(r)\dagger}(j_1 j_2), \quad (6)$$

and we assume  $A^{(r)\dagger} = \sum_{j_1 j_2} y(j_1 j_2 r) A^{(r)\dagger}(j_1 j_2)$  with  $y(j_1 j_2 r) = c(j_1 j_2)$ . For the eight open-shell nuclei  $^{128,126,124,122}\text{Cd}$  and  $^{132,134,136,138}\text{Cd}$ , the structures of valence-proton-hole pairs and those of valence-neutron-hole/-particle pairs are determined separately as above.

## B. Shell-model Hamiltonians

For  $^{130,132,134,136,138}\text{Cd}$ , we consider valence proton holes in the 28-50 major shell and valence neutron particles in the 82-126 major shell. The SM effective Hamiltonian  $jj46$  of Ref. [23] is adopted. To be specific, based on the Pandya transformation [57], we derive the effective Hamiltonian for valence proton holes and neutron particles with respect to the core of  $Z = 50$  and  $N = 82$  as follows, from the  $jj46$  Hamiltonian [23] for valence proton and neutron particles with respect to the core of  $Z = 28$  and  $N = 82$ :

and  $10_1^+$  states of these four Cd nuclei:

$$\begin{aligned} H &= H_\pi + H_\nu + H_{\pi\nu}, \\ H_\pi &= \sum_{j_\pi} \varepsilon_{j_\pi} \hat{n}_{j_\pi} + \sum_{s=0,2,8} G_\pi^s [P_\pi^{(s)\dagger} \cdot \tilde{P}_\pi^{(s)}] \\ &\quad + \kappa_\pi [Q^{(2)}(\pi) \cdot Q^{(2)}(\pi)], \\ H_\nu &= \sum_{j_\nu} \varepsilon_{j_\nu} \hat{n}_{j_\nu} + \sum_{s=0,2,10} G_\nu^s [P_\nu^{(s)\dagger} \cdot \tilde{P}_\nu^{(s)}] \\ &\quad + \kappa_\nu [Q^{(2)}(\nu) \cdot Q^{(2)}(\nu)], \\ H_{\pi\nu} &= \kappa_{\pi\nu} [Q^{(2)}(\pi) \cdot Q^{(2)}(\nu)], \end{aligned} \quad (8)$$

with the operators defined as below,

$$\begin{aligned} \hat{n}_j &= \sum_m a_{jm}^\dagger a_{jm}, \\ P^{(0)\dagger} &= \sum_j \frac{\sqrt{2j+1}}{2} (a_j^\dagger \times a_j^\dagger)^{(0)}, \end{aligned}$$

TABLE I. Hamiltonian parameters adopted for  $^{128,126,124,122}\text{Cd}$ . The single-proton-hole and single-neutron-hole energies, i.e.,  $\varepsilon_{j_\pi}$  and  $\varepsilon_{j_\nu}$ , are taken to be the excitation energies of the single-proton-hole states of  $^{131}\text{In}$  [23,59,60] and those of the single-neutron-hole states of  $^{131}\text{Sn}$  [59], respectively. The interaction strength parameters are adjusted to fit the experimental energy levels of the four nuclei.  $G_\tau^0$  (in units of MeV),  $G_\tau^2$  (in units of MeV/ $r_0^4$ ) and  $\kappa_\tau$  (in units of MeV/ $r_0^4$ ) with  $\tau = \pi, \nu$ , as well as  $\kappa_{\pi\nu}$  (in units of MeV/ $r_0^4$ ), are set to remain the same for the four nuclei; the strength parameter for the proton-hole highest-spin pairing interaction with spin 8 is set to be  $G_\pi^8 = 1.8 \times 10^{-6}$  MeV/ $r_0^4$ , and the strength parameter for the neutron-hole highest-spin pairing interaction with spin 10 is set to be  $G_\nu^{10} = (-4.764252e^{-N_n} + 0.943860) \times 10^{-8}$  MeV/ $r_0^4$  with  $N_n = 2, 4, 6, 8$  for  $^{128,126,124,122}\text{Cd}$ .

	$\pi f_{5/2}$	$\pi p_{3/2}$	$\pi p_{1/2}$	$\pi g_{9/2}$		
$\varepsilon$	2.750	1.353	0.302	0.000		
	$\nu g_{7/2}$	$\nu d_{5/2}$	$\nu d_{3/2}$	$\nu s_{1/2}$	$\nu h_{11/2}$	
$\varepsilon$	2.434	1.655	0.000	0.332	0.242	
$G_\pi^0$	$G_\pi^2$	$\kappa_\pi$	$G_\nu^0$	$G_\nu^2$	$\kappa_\nu$	$\kappa_{\pi\nu}$
-0.195	-0.055	-0.085	-0.140	-0.020	-0.045	-0.080

$$P^{(\lambda)\dagger} = \sum_{j_1 j_2} q(j_1 j_2 \lambda) (a_{j_1}^\dagger \times a_{j_2}^\dagger)^{(\lambda)}, \quad \lambda \neq 0,$$

$$Q^{(2)} = \sum_{j_1 j_2} q(j_1 j_2 2) (a_{j_1}^\dagger \times \tilde{a}_{j_2})^{(2)},$$

$$q(j_1 j_2 \lambda) = -\frac{(j_1 \| r^\lambda Y^{(\lambda)} \| j_2)}{\hat{\lambda}}. \quad (9)$$

Here  $Q^{(2)}$  is the quadrupole operator defined in Eq. (1), with its form in the second-quantization representation;  $\tilde{a}_{jm}$  is the time-reversed operator of a single-particle destruction, and we use the convention  $\tilde{a}_{jm} = (-)^{j-m} a_{j,-m}$ ;  $(j_1 \| r^\lambda Y^{(\lambda)} \| j_2)$  is the reduced matrix element, and we use the Edmond convention [58];  $\hat{\lambda} = \sqrt{2\lambda + 1}$ . The single-proton-hole energies  $\varepsilon_{j_\pi}$  and single-neutron-hole energies  $\varepsilon_{j_\nu}$  are taken to be the excitation energies of the single-proton-hole states of  $^{131}\text{In}$  [23,59,60] and those of the single-neutron-hole states of  $^{131}\text{Sn}$  [59], respectively. The strength parameters,  $G_\tau^0$ ,  $G_\tau^2$ , and  $\kappa_\tau$  with

$\tau = \pi, \nu$ , as well as  $G_\pi^8$ ,  $G_\nu^{10}$ , and  $\kappa_{\pi\nu}$ , are adjusted to fit the experimental energy levels of the four Cd nuclei. In Table I we list the parameters adopted in this work.

### III. RESULTS AND DISCUSSIONS

For  $^{128,126,124,122}\text{Cd}$  we perform the NPA calculation using the phenomenological Hamiltonian as described in Sec. II. The pair configuration spaces are constructed using *SDGI* pairs (with spin 0,2,4,6) of proton holes and those of neutron holes. The proton-hole highest-spin pair  $(0g_{9/2} \times 0g_{9/2})^{(8)}$  and neutron-hole highest-spin pair  $(0h_{11/2} \times 0h_{11/2})^{(10)}$  are also adopted, which, together with the proton-hole spin-8 pairing interaction and neutron-hole spin-10 pairing interaction additionally included in the phenomenological Hamiltonian, are essential to provide a good description of the  $8_1^+$  and  $10_1^+$  states of these four Cd nuclei.

For  $^{130,132,134,136,138}\text{Cd}$  we use the effective interaction *jj46* of Ref. [23]. Our configuration spaces are constructed using *SDGI* pairs of proton holes and those of neutron particles. We also adopt the proton-hole highest-spin pair  $(0g_{9/2} \times 0g_{9/2})^{(8)}$ . In Ref. [36] it was shown that for the low-lying states of  $^{132}\text{Cd}$  and  $^{130}\text{Pd}$ , the SM wave function can be approximately represented by one optimized pair basis state constructed by coupled pairs adopted here.

In Figs. 1 and 2 we present the calculated excitation energies of the low-lying states for  $^{128,126,124,122}\text{Cd}$  and  $^{130,132,134,136,138}\text{Cd}$ , in comparison with available experimental data [20,49,59,61–63]. In Fig. 3, for the nine Cd nuclei, we present in the upper panel the calculated excitation energies of the  $2_1^+$  and  $4_1^+$  states and in the lower panel the calculated  $R_{4/2}$  value, versus the mass number  $A$ , as well as available experimental results. For  $^{128,126,124,122}\text{Cd}$ , in Fig. 1 one sees that the calculated results well reproduce the experimental data, except for the  $2_2^+$  state of  $^{126}\text{Cd}$ . For  $^{130,132,134,136,138}\text{Cd}$ , only the low-lying yrast states of  $^{130}\text{Cd}$ , as well as the  $2_1^+$  state of  $^{132}\text{Cd}$ , were studied experimentally [20,49], and their excitation energies are well reproduced by our NPA calculation using the *jj46* interaction as shown in Fig. 2. Note that for semimagic  $^{130}\text{Cd}$  with two valence proton holes, the NPA results are exactly the same as those given by the SM.

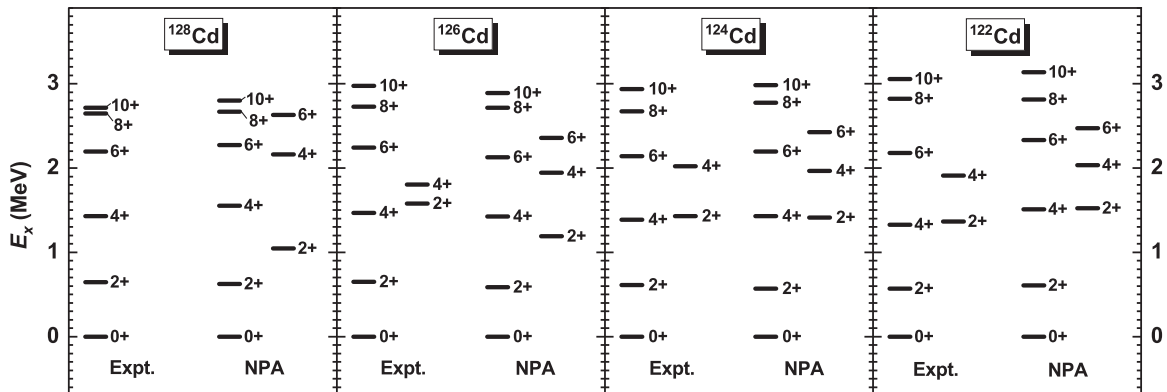


FIG. 1. The excitation energies (denoted as  $E_x$ , in units of MeV) of the low-lying states for  $^{128,126,124,122}\text{Cd}$  given by our NPA calculation, in comparison with experimental data [59,61–63].

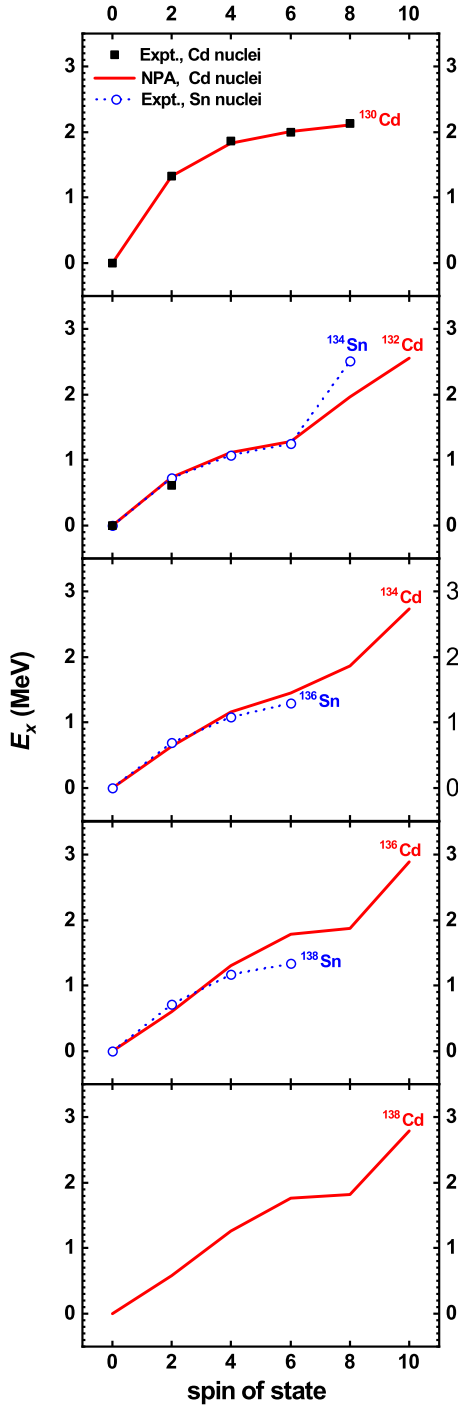


FIG. 2. The excitation energies (denoted as  $E_x$ , in units of MeV) of the low-lying yrast states for  $^{130,132,134,136,138}\text{Cd}$  given by our NPA calculation using the  $jj46$  effective interaction of Ref. [23], in comparison with available experimental data [20,49]. We also present the experimental excitation energies of corresponding semimagic Sn nuclei [59,64] for comparison.

For the low-lying yrast states of  $^{128}\text{Cd}$  and  $^{132}\text{Cd}$  we also perform SM calculations, i.e., calculations in the full valence spaces. In Fig. 4 we present the overlaps between the SM wave functions obtained in the full spaces and corresponding NPA

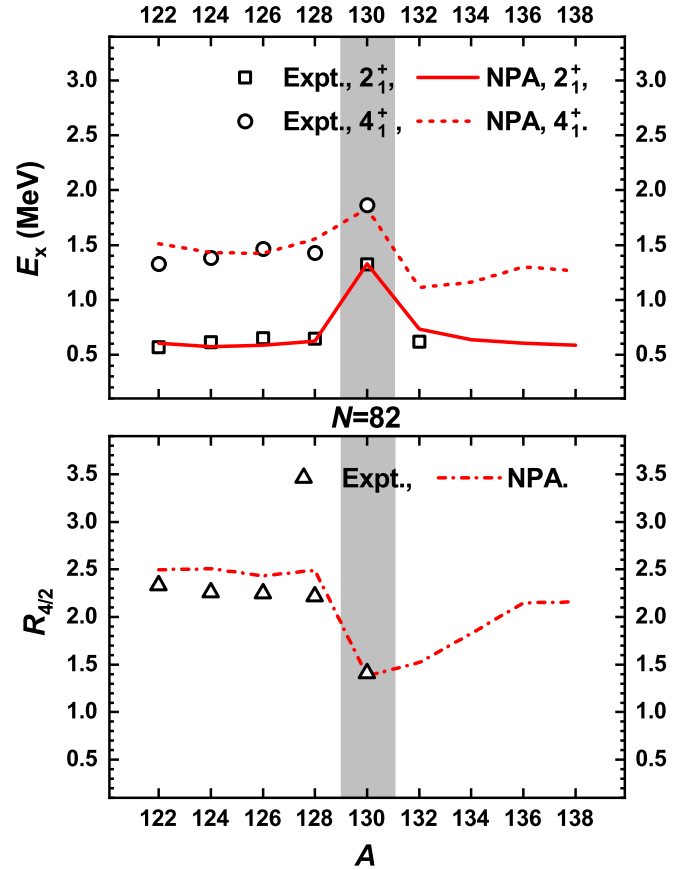


FIG. 3. The excitation energies of the  $2_1^+$  and  $4_1^+$  states in the upper panel and the  $R_{4/2}$  value in the lower panel, versus the mass number  $A$ , for the nine Cd nuclei.

wave functions obtained in the pair-truncated subspaces. One sees the overlaps are all very close to 1.

For  $^{128,126,124,122}\text{Cd}$ , as shown in Fig. 1 the excitation energies of the  $2_1^+$  states, as well as those of the  $4_1^+$  states, are close to each other. Correspondingly, the  $R_{4/2}$  values of the four nuclei are close to each other, and  $\approx 2.5$  is given by our NPA calculation. For  $^{130,132,134,136,138}\text{Cd}$ , in Fig. 2 we also present the available experimental excitation energies of corresponding semimagic Sn nuclei [59,64] for comparison. One sees that our calculated excitation energies of corresponding states of  $^{132}\text{Cd}$  are very close to the experimental excitation energies of corresponding states of  $^{134}\text{Sn}$ . This is consistent with the results of Ref. [36], where it was shown that the SM wave functions of the  $0_{g.s.}^+$ ,  $2_1^+$ ,  $4_1^+$ ,  $6_1^+$  states of  $^{132}\text{Cd}$  are dominated by the pair basis states  $(|S\rangle_\pi \times |S\rangle_\nu)^{(0)}$ ,  $(|S\rangle_\pi \times |D\rangle_\nu)^{(2)}$ ,  $(|S\rangle_\pi \times |G\rangle_\nu)^{(4)}$ ,  $(|S\rangle_\pi \times |I\rangle_\nu)^{(6)}$ , respectively. These indicate that the lowest-seniority scheme works in low-lying states of  $^{132}\text{Cd}$ . Yet, as shown in Fig. 2, at  $^{134}\text{Cd}$  the  $E_x$  curve starts to deviate from that of the corresponding Sn nucleus, and the deviation becomes considerable for the case of  $^{136}\text{Cd}$ . For  $^{132,134,136}\text{Cd}$ , we calculate the overlap between the NPA wave function of the  $0_{g.s.}^+$  state and the  $S$ -pair-condensate state, and the overlap between the NPA wave function of the low-lying excited state of spin  $J$  and the generalized-seniority-2 state with one broken neutron pair of spin  $J$ . The overlaps

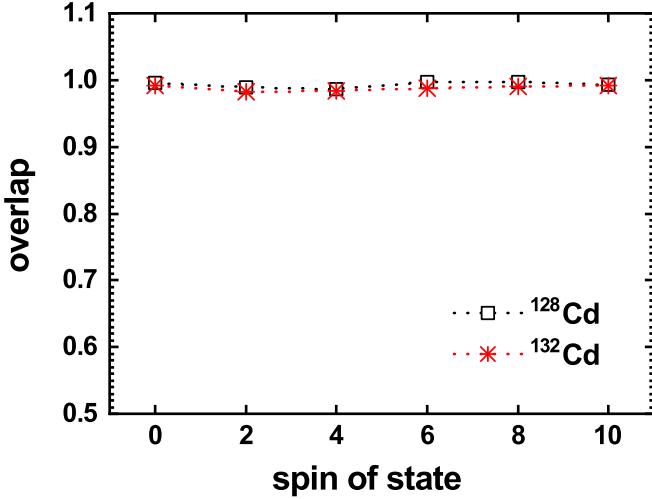


FIG. 4. The overlaps between the SM wave functions obtained in the full valence spaces and corresponding NPA wave functions obtained in the pair-truncated subspaces, for the low-lying yrast states of  $^{128}\text{Cd}$  and  $^{132}\text{Cd}$ .

regarding the  $0_{\text{g.s.}}^+$  states are 0.97, 0.91, 0.87; those regarding the  $2_1^+$  states are 0.91, 0.77, 0.68; those regarding the  $4_1^+$  states are 0.94, 0.47, 0.21; those regarding the  $6_1^+$  states are 0.96, 0.87, 0.54. In Fig. 3 one sees that the  $R_{4/2}$  values are increasing gradually from  $\approx 1.5$  to  $\approx 2.1$  for  $^{132,134,136}\text{Cd}$ . These together reflect that for  $^{132,134,136}\text{Cd}$  there is a gradual change from the lowest-seniority scheme to the spherical-vibrator scheme. For  $^{138}\text{Cd}$ , the  $E_x$  curve and the  $R_{4/2}$  value are very similar to those of  $^{136}\text{Cd}$ .

In Table II we present our calculated quadrupole transition probabilities  $B(E2)$  of the  $2_1^+ \rightarrow 0_{\text{g.s.}}^+$ ,  $4_1^+ \rightarrow 2_1^+$ ,  $6_1^+ \rightarrow 4_1^+$  transitions for the nine Cd nuclei. Regarding the effective charges, for  $^{122,124,126,128}\text{Cd}$  we adopt  $e_\pi = -1.65$  for valence proton holes and  $e_\nu = -0.95$  for valence neutron holes, which are optimized with respect to the available experimental  $B(E2)$  values [22]; for  $^{130,132,134,136,138}\text{Cd}$  we adopt  $e_\pi = -1.70$  for valence proton holes and  $e_\nu = 0.70$  for valence neutron particles, which are taken from Ref. [23] together with the  $jj46$  effective interaction.

In the upper panel of Fig. 5 we present our calculated  $B(E2; 0_{\text{g.s.}}^+ \rightarrow 2_1^+)$  values, versus the mass number  $A$ , as well as the available experimental values of  $B(E2; 0_{\text{g.s.}}^+ \rightarrow 2_1^+)$  [22]. One sees that our calculated results reproduce the experimental data very well. Note that the  $B(E2; 0_{\text{g.s.}}^+ \rightarrow 2_1^+)$  value is equal to the corresponding  $B(E2; 2_1^+ \rightarrow 0_{\text{g.s.}}^+)$  value multiplied by a factor of 5. For comparison, we also present the theoretical  $B(E2; 0_{\text{g.s.}}^+ \rightarrow 2_1^+)$  results given by the SM calculation [22], those by the beyond-mean-field calculation [2], and those by the QRPA calculation including the phonon-phonon coupling [4]. As shown in Fig. 5, for  $^{122,124,126,128}\text{Cd}$  our NPA results are close to those given by the beyond-mean-field calculation; for  $^{124,126}\text{Cd}$  our results are also close to the available SM results. From  $^{126}\text{Cd}$  to  $^{134}\text{Cd}$ , the  $B(E2; 0_{\text{g.s.}}^+ \rightarrow 2_1^+)$  values given by our NPA calculation, as well as the curvature

TABLE II. Calculated quadrupole transition probabilities  $B(E2)$  (in units of  $e^2\text{fm}^4$ ) of the  $2_1^+ \rightarrow 0_{\text{g.s.}}^+$ ,  $4_1^+ \rightarrow 2_1^+$ ,  $6_1^+ \rightarrow 4_1^+$  transitions for the nine Cd nuclei, in comparison with available experimental data [22].

Nuclei	$J_i$	$J_f$	$B^{\text{NPA}}(E2)$	$B^{\text{Expt.}}(E2)$
$^{122}\text{Cd}$	$2_1^+$	$0_1^+$	690.4	820 (400)
	$4_1^+$	$2_1^+$	903.5	
	$6_1^+$	$4_1^+$	416.7	
$^{124}\text{Cd}$	$2_1^+$	$0_1^+$	632.6	700 (380)
	$4_1^+$	$2_1^+$	797.4	
	$6_1^+$	$4_1^+$	411.7	
$^{126}\text{Cd}$	$2_1^+$	$0_1^+$	535.9	540 (120)
	$4_1^+$	$2_1^+$	659.0	
	$6_1^+$	$4_1^+$	409.4	
$^{128}\text{Cd}$	$2_1^+$	$0_1^+$	368.9	
	$4_1^+$	$2_1^+$	415.6	
	$6_1^+$	$4_1^+$	137.0	
$^{130}\text{Cd}$	$2_1^+$	$0_1^+$	180.9	
	$4_1^+$	$2_1^+$	206.7	
	$6_1^+$	$4_1^+$	146.2	
$^{132}\text{Cd}$	$2_1^+$	$0_1^+$	206.8	
	$4_1^+$	$2_1^+$	185.2	
	$6_1^+$	$4_1^+$	105.3	
$^{134}\text{Cd}$	$2_1^+$	$0_1^+$	379.7	
	$4_1^+$	$2_1^+$	388.2	
	$6_1^+$	$4_1^+$	120.0	
$^{136}\text{Cd}$	$2_1^+$	$0_1^+$	532.9	
	$4_1^+$	$2_1^+$	645.1	
	$6_1^+$	$4_1^+$	251.1	
$^{138}\text{Cd}$	$2_1^+$	$0_1^+$	635.7	
	$4_1^+$	$2_1^+$	761.5	
	$6_1^+$	$4_1^+$	502.8	

when crossing the  $N = 82$  shell closure, are similar to those given by the QRPA calculation.

Interestingly, one sees in the upper panel of Fig. 5 that our calculated  $B(E2; 0_{\text{g.s.}}^+ \rightarrow 2_1^+)$  values exhibit an asymmetric feature with respect to the  $N = 82$  shell closure, i.e., the  $B(E2; 0_{\text{g.s.}}^+ \rightarrow 2_1^+)$  value of the neutron-particle Cd nucleus with  $N = 82 + N_n$  is smaller than that of corresponding neutron-hole Cd nucleus with  $N = 82 - N_n$ , for all the four cases of  $N_n = 2, 4, 6, 8$ . One also sees that the  $B(E2; 0_{\text{g.s.}}^+ \rightarrow 2_1^+)$  values given by the QRPA calculation including the phonon-phonon coupling [4] have a similar asymmetric character, for the cases of  $N_n = 2$  and 4. In recent years, the asymmetric feature of  $B(E2; 0_{\text{g.s.}}^+ \rightarrow 2_1^+)$  for Sn isotopes (with  $Z = 50$ ) with respect to half of the  $N = 50-82$  major shell, as well as that for Te isotopes (with  $Z = 52$ ), has been extensively discussed; see, e.g., Refs. [34,65–67].

Below we study this asymmetric feature of the quadrupole transition probability  $B(E2; 0_{\text{g.s.}}^+ \rightarrow 2_1^+)$ , in terms of corresponding proton and neutron transition matrix elements  $M_\pi$  and  $M_\nu$ . The relation between the  $B(E2)$  value

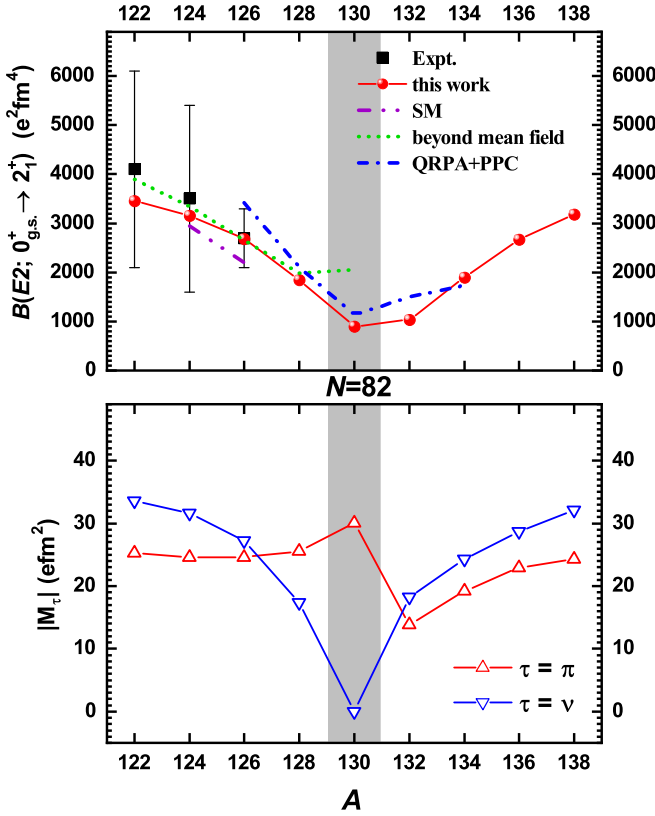


FIG. 5. Our calculated quadrupole transition probability  $B(E2; 0_{g.s.}^+ \rightarrow 2_1^+)$ , as well as available experimental data [22], in the upper panel, and the absolute values of corresponding proton and neutron transition matrix elements  $M_{\pi}$  and  $M_{\nu}$  in the lower panel, versus the mass number  $A$ . According to our calculation, for  $^{128,126,124,122}\text{Cd}$  and  $^{132,134,136,138}\text{Cd}$ , the  $M_{\pi}/M_{\nu}$  values are all positive, i.e., the contributions of  $M_{\pi}$  and  $M_{\nu}$  in  $B(E2; 0_{g.s.}^+ \rightarrow 2_1^+)$  are added up for all these eight Cd nuclei. For comparison, we also present in the upper panel the theoretical  $B(E2; 0_{g.s.}^+ \rightarrow 2_1^+)$  results given by the SM calculation [22], those by the beyond-mean-field calculation [2], and those by the QRPA calculation including the phonon-phonon coupling [4]. See text for details.

and corresponding  $M_{\pi}$  and  $M_{\nu}$  values is

$$B(E2; \alpha_i J_i \rightarrow \alpha_f J_f) = \frac{1}{2J_i + 1} |M_{\pi} + M_{\nu}|^2, \quad (10)$$

$$M_{\tau} = (\alpha_f J_f || e_{\tau} Q^{(2)}(\tau) || \alpha_i J_i), \quad \tau = \pi, \nu,$$

where  $Q^{(2)}(\tau)$  is given in Eq. (1), and the subscripts “f” and “i” are used to denote the final and initial low-lying states, respectively. In the lower panel of Fig. 5, we present the absolute values of  $M_{\pi}$  and  $M_{\nu}$  for the nine Cd nuclei. According to our calculation, for  $^{128,126,124,122}\text{Cd}$  and  $^{132,134,136,138}\text{Cd}$ , the  $M_{\pi}/M_{\nu}$  values are all positive, i.e., the contributions of  $M_{\pi}$  and  $M_{\nu}$  in  $B(E2; 0_{g.s.}^+ \rightarrow 2_1^+)$  are added up for all these

eight open-shell Cd nuclei. As shown in the lower panel of Fig. 5, the  $M_{\nu}$  values are almost symmetric with respect to the  $N = 82$  shell closure, while the  $M_{\pi}$  values for  $^{128,126,124,122}\text{Cd}$  are  $\approx 25 e\text{fm}^2$ , and those for  $^{132,134,136,138}\text{Cd}$  are smaller, from  $\approx 14$  to  $\approx 24 e\text{fm}^2$ . In addition, one sees that for the case of  $N_n = 2$  the two  $B(E2; 0_{g.s.}^+ \rightarrow 2_1^+)$  values are most asymmetric; meanwhile, the two  $M_{\nu}$  values are almost the same while the two  $M_{\pi}$  values are very different from each other. Thus we conclude that this asymmetric feature of the  $B(E2; 0_{g.s.}^+ \rightarrow 2_1^+)$  values with respect to the  $N = 82$  shell closure mainly comes from the contributions of the proton transition matrix elements. As also shown in the lower panel of Fig. 5, it is interesting that the  $M_{\pi}$  value for  $^{130}\text{Cd}$  with  $N = 82$  is close to those for  $^{128,126,124,122}\text{Cd}$ , and with two more neutrons outside  $^{130}\text{Cd}$  the  $M_{\pi}$  value has a considerable decrease.

At last we investigate for  $^{128,126,124,122}\text{Cd}$  and  $^{132,134,136,138}\text{Cd}$ , whether two low-lying yrast states with spins differing by 2 can be connected by the quadrupole-phonon excitation. We calculate explicit overlaps between the low-lying yrast states and the constructed phonon states, denoted as  $\langle \psi_f | \phi_i^{(J_f)}(\tau) \rangle$  with the low-lying state  $|\psi_f\rangle = |\alpha_f J_f M_f\rangle$  and the phonon state

$$|\phi_i^{(J_f)}(\tau)\rangle = \frac{1}{\mathcal{N}} \sum_{\kappa, M_i} C_{2\kappa J_i M_i}^{J_f M_f} \frac{Q_{\kappa}^{(2)}(\tau)}{r_0^2} |\alpha_i J_i M_i\rangle, \quad (11)$$

where the quadrupole operator  $Q^{(2)}(\tau)$  is defined in Eq. (1), and  $\frac{1}{\mathcal{N}}$  is the normalization factor. Here we take  $|\psi_f\rangle = |I_1^+\rangle$  and  $|\psi_i\rangle = |(I - 2)_1^+\rangle$ , and in Fig. 6 we present corresponding overlaps for  $^{128,126,124,122}\text{Cd}$  and  $^{132,134,136,138}\text{Cd}$ . One sees that, for all eight open-shell Cd nuclei,  $|2_1^+\rangle$  and  $|4_1^+\rangle$  can be well described to be the states obtained by coupling the proton or neutron quadrupole phonon to  $|0_{g.s.}^+\rangle$  and  $|2_1^+\rangle$ , respectively, with the overlaps approximately equal to or larger than 0.8. In other words, for all eight Cd nuclei, the connection between  $|2_1^+\rangle$  and  $|0_{g.s.}^+\rangle$  and that between  $|4_1^+\rangle$  and  $|2_1^+\rangle$ , are dominated by the proton or neutron quadrupole phonon excitation.

In Fig. 6 one also sees that, interestingly, for  $^{126,124,122}\text{Cd}$  and  $^{136,138}\text{Cd}$ , the overlap between the  $2_1^+$  state and the proton phonon state  $|\phi_{g.s.}^{(2)}(\pi)\rangle$  obtained by coupling the proton phonon to the  $0_{g.s.}^+$  state, and the overlap between the  $2_1^+$  state and the neutron phonon state  $|\phi_{g.s.}^{(2)}(\nu)\rangle$  obtained by coupling the neutron phonon to the  $0_{g.s.}^+$  state, are both around 0.8. In other words, the  $2_1^+$  state of these nuclei can be well described to be both the proton phonon state and the neutron phonon state. This indicates that the two phonon states are not orthogonal, i.e., the overlap  $\langle \phi_{g.s.}^{(2)}(\pi) | \phi_{g.s.}^{(2)}(\nu) \rangle$  does not vanish. As follows, we have an analytic relation for this overlap in terms of the expectations of the proton-neutron, proton-proton, and neutron-neutron quadrupole-quadrupole operators in the  $0_{g.s.}^+$  state:

$$\langle \phi_{g.s.}^{(2)}(\pi) | \phi_{g.s.}^{(2)}(\nu) \rangle = \frac{\langle 0_{g.s.}^+ | Q^{(2)}(\pi) \cdot Q^{(2)}(\nu) | 0_{g.s.}^+ \rangle}{\sqrt{\langle 0_{g.s.}^+ | Q^{(2)}(\pi) \cdot Q^{(2)}(\pi) | 0_{g.s.}^+ \rangle \langle 0_{g.s.}^+ | Q^{(2)}(\nu) \cdot Q^{(2)}(\nu) | 0_{g.s.}^+ \rangle}}. \quad (12)$$

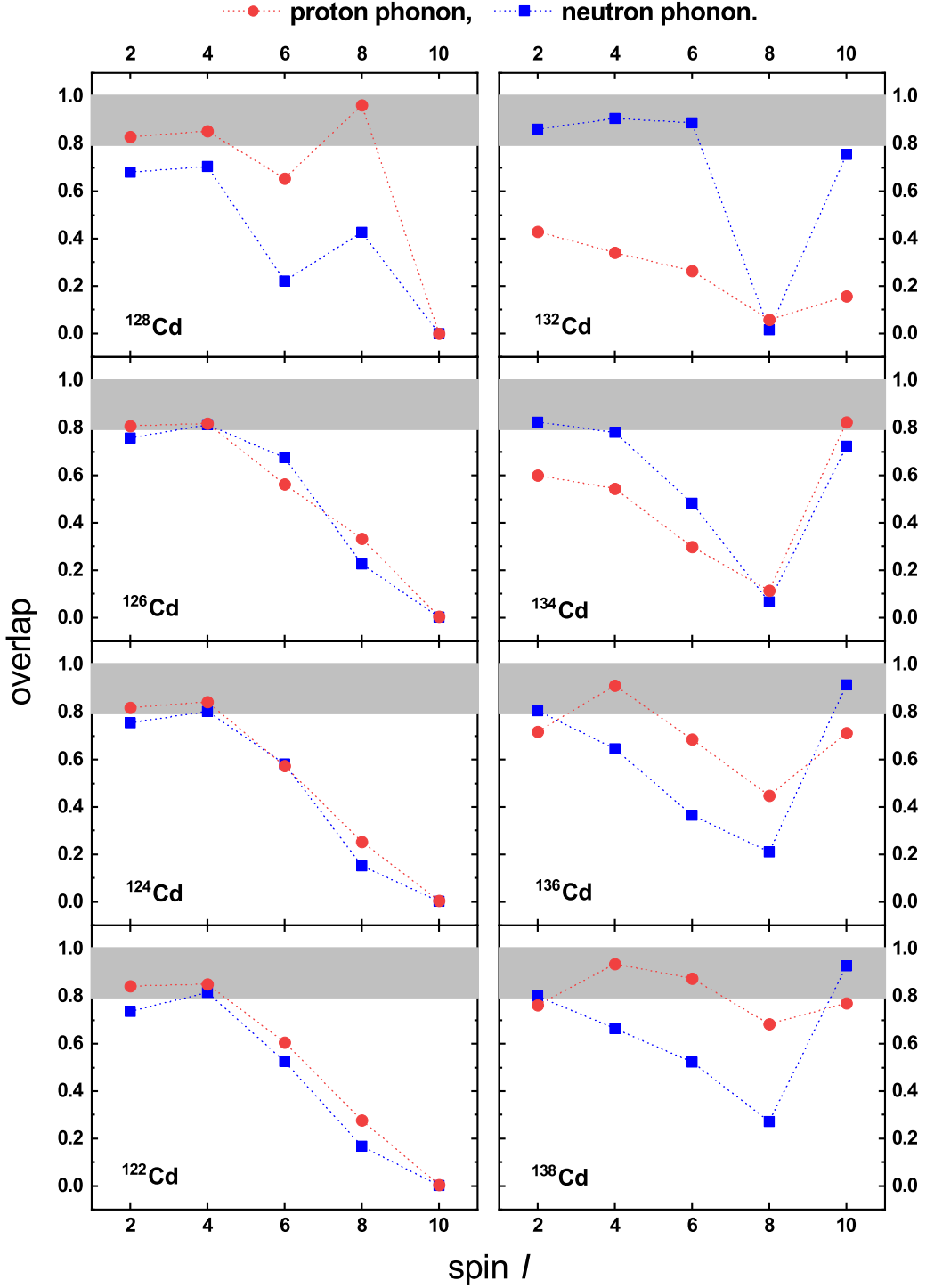


FIG. 6. The explicit overlap between the low-lying yrast state with spin  $I$  and the phonon state constructed by coupling the proton or neutron quadrupole phonon, i.e.,  $\frac{Q^{(2)}(\tau)}{r_0^2}$  with  $\tau = \pi$  or  $\nu$ , to the yrast state with spin  $(I - 2)$ . See text for details.

This relation implies that, in an open-shell nucleus, the two phonon states  $|\phi_{\text{g.s.}}^{(2)}(\pi)\rangle$  and  $|\phi_{\text{g.s.}}^{(2)}(\nu)\rangle$  are almost impossibly orthogonal, due to the essential role played by the proton-neutron quadrupole-quadrupole interaction in the  $0_{\text{g.s.}}^+$  state. For  $^{128,126,124,122}\text{Cd}$  the overlap  $\langle\phi_{\text{g.s.}}^{(2)}(\pi)|\phi_{\text{g.s.}}^{(2)}(\nu)\rangle$ , i.e., the ratio between the expectation of the proton-neutron quadrupole-quadrupole operator in the  $0_{\text{g.s.}}^+$  state and the ge-

ometric mean value of the expectations of the proton-proton and neutron-neutron quadrupole-quadrupole operators in the  $0_{\text{g.s.}}^+$  state, equals 0.25, 0.34, 0.38, 0.38, respectively, and for  $^{132,134,136,138}\text{Cd}$  this overlap equals  $-0.18$ ,  $-0.28$ ,  $-0.35$ ,  $-0.38$ , respectively.

It is also worthwhile to note that the overlap  $\langle\psi_{\text{f}}|\phi_{\text{i}}^{(J_f)}(\tau)\rangle$  depends on the wave-function details of the initial and final



states, which we take to be the low-lying yrast states with spins differing by 2 in this work. Then the two curves of the overlaps with  $\tau = \pi$  and  $\nu$ , respectively, in each panel of Fig. 6, reflect the structure evolution along the yrast line. In this regard Fig. 6 might indicate that  $^{126}\text{Cd}$ ,  $^{124}\text{Cd}$ ,  $^{122}\text{Cd}$  have similar structure evolutions along the yrast lines, and so do the  $^{136}\text{Cd}$  and  $^{138}\text{Cd}$  nuclei.

#### IV. SUMMARY

In this paper we study the low-lying states of neutron-rich  $^{122,124,126,128}\text{Cd}$  and  $^{130,132,134,136,138}\text{Cd}$  within the nucleon-pair approximation (NPA) of the shell model. For  $^{122,124,126,128}\text{Cd}$  we adopt the phenomenological Hamiltonian including monopole pairing, quadrupole pairing, quadrupole-quadrupole interactions, as well as the proton-hole highest-spin pairing interaction with spin 8 and the neutron-hole highest-spin pairing interaction with spin 10; and for  $^{130,132,134,136,138}\text{Cd}$  we adopt the effective interaction  $jj46$  [23]. The available experimental excitation energies and quadrupole transition probabilities for the low-lying states are well reproduced by our calculation, and we also make predictions for the low-lying states of very neutron-rich Cd nuclei up to  $^{138}\text{Cd}$ .

We study the evolution of the quadrupole transition probability  $B(E2; 0_{\text{g.s.}}^+ \rightarrow 2_1^+)$  from  $^{122}\text{Cd}$  to  $^{138}\text{Cd}$ , in terms of corresponding proton and neutron transition matrix elements  $M_\pi$  and  $M_\nu$ . Based on our calculation, the  $B(E2; 0_{\text{g.s.}}^+ \rightarrow 2_1^+)$  values exhibit an asymmetric feature with respect to the  $N = 82$  shell closure, which mainly comes from the contributions of the proton transition matrix elements.

For the eight open-shell Cd nuclei, we investigate whether the low-lying yrast states with spin  $I$  can be interpreted to be the phonon states obtained by coupling the proton or neutron phonon to the low-lying yrast states with spin  $(I - 2)$ , and here we take the proton or neutron quadrupole operators multiplied by  $1/r_0^2$  for our phonon operators. We calculate explicit overlaps between the yrast states and the constructed phonon states, and the results indicate that, for all eight open-shell Cd nuclei,  $|2_1^+\rangle$  and  $|4_1^+\rangle$  can be well described as the phonon states constructed by coupling the proton or neutron phonon to  $|0_{\text{g.s.}}^+\rangle$  and  $|2_1^+\rangle$ , respectively.

Very interestingly, for  $^{126,124,122}\text{Cd}$  and  $^{136,138}\text{Cd}$ , the  $2_1^+$  state can be well described to be both the proton phonon state and the neutron phonon state, which indicates a nonorthogonal feature of these two phonon states. We further present an analytic relation for the overlap between these two phonon states. This relation implies that the proton and neutron phonon states constructed using the quadrupole operators and the  $0_{\text{g.s.}}^+$  state in an open-shell nucleus are almost impossibly orthogonal, due to the essential role played by the proton-neutron quadrupole-quadrupole interaction in the  $0_{\text{g.s.}}^+$  state.

For future work, the optimization of the quadrupole-phonon structure, with respect to the NPA wave functions of the initial and final states, will be of much interest.

#### ACKNOWLEDGMENTS

We are grateful to Prof. Yu-Min Zhao and Prof. Mark Caprio for helpful discussions. Dr. Cenxi Yuan is gratefully acknowledged for providing the  $jj46$  effective interaction. We thank the National Natural Science Foundation of China (Grants No. 11875134 and No. 11775081) for financial support.

- 
- [1] A. Bohr and B. R. Mottelson, *Nuclear Structure: II Nuclear Deformations* (Benjamin, New York, 1975).
  - [2] T. R. Rodríguez, J. Luis Egido, and A. Jungclauss, *Phys. Lett. B* **668**, 410 (2007).
  - [3] P. Fleischer, P. Klüpfel, P.-G. Reinhard, and J. A. Maruhn, *Phys. Rev. C* **70**, 054321 (2004).
  - [4] A. P. Severyukhin, N. N. Arsenyev, I. N. Borzov, and E. O. Sushenok, *Phys. Rev. C* **95**, 034314 (2017).
  - [5] A. Arima and F. Iachello, *Phys. Rev. Lett.* **35**, 1069 (1975); *Ann. Phys. (N.Y.)* **99**, 253 (1976); **111**, 201 (1978); **123**, 468 (1979); *Adv. Nucl. Phys.* **13**, 139 (1984).
  - [6] K. Heyde, P. Van Isacker, M. Waroquier, G. Wenes, and M. Sambataro, *Phys. Rev. C* **25**, 3160 (1982).
  - [7] M. Délèze, S. Drissi, J. Kern, P. A. Tercier, J. P. Vorlet, J. Rikowska, T. Otsuka, S. Judge, and A. Williams, *Nucl. Phys. A* **551**, 269 (1993).
  - [8] R. F. Casten, J. Jolie, H. G. Börner, D. S. Brenner, N. V. Zamfir, W. T. Chou, and A. Aprahamian, *Phys. Lett. B* **297**, 19 (1992).
  - [9] M. Kadi, N. Warr, P. E. Garrett, J. Jolie, and S. W. Yates, *Phys. Rev. C* **68**, 031306(R) (2003).
  - [10] P. E. Garrett, K. L. Green, H. Lehmann, J. Jolie, C. A. McGrath, M. Yeh, and S. W. Yates, *Phys. Rev. C* **75**, 054310 (2007).
  - [11] P. E. Garrett, K. L. Green, and J. L. Wood, *Phys. Rev. C* **78**, 044307 (2008).
  - [12] A. Leviatan, N. Gavrielov, J. E. García-Ramos, and P. Van Isacker, *Phys. Rev. C* **98**, 031302(R) (2018).
  - [13] C. Qi, J. Blomqvist, T. Bäck, B. Cederwall, A. Johnson, R. J. Liotta, and R. Wyss, *Phys. Rev. C* **84**, 021301(R) (2011).
  - [14] S. Zerguine and P. Van Isacker, *Phys. Rev. C* **83**, 064314 (2011).
  - [15] P. Van Isacker, A. O. Macchiavelli, P. Fallon, and S. Zerguine, *Phys. Rev. C* **94**, 024324 (2016).
  - [16] P. Van Isacker, J. Engel, and K. Nomura, *Phys. Rev. C* **96**, 064305 (2017).
  - [17] G. J. Fu, J. J. Shen, Y. M. Zhao, and A. Arima, *Phys. Rev. C* **87**, 044312 (2013).
  - [18] G. J. Fu, Y. M. Zhao, and A. Arima, *Phys. Rev. C* **97**, 024337 (2018).
  - [19] I. Dillmann, K.-L. Kratz, A. Wöhr, O. Arndt, B. A. Brown, P. Hoff, M. Hjorth-Jensen, U. Köster, A. N. Ostrowski, B. Pfeiffer, D. Seweryniak, J. Shergur, and W. B. Walters, *Phys. Rev. Lett.* **91**, 162503 (2003).
  - [20] A. Jungclauss, L. Cáceres, M. Górska, M. Pfützner, S. Pietri, E. Werner-Malento, H. Grawe, K. Langanke, G. Martínez-Pinedo, F. Nowacki, A. Poves, J. J. Cuenca-García, D. Rudolph, Z. Podolyak, P. H. Regan, P. Detistov, S. Lalkovski, V.

- Modamio, J. Walker, P. Bednarczyk *et al.*, *Phys. Rev. Lett.* **99**, 132501 (2007).
- [21] H. Watanabe, G. Lorusso, S. Nishimura, Z. Y. Xu, T. Sumikama, P.-A. Söderström, P. Doornenbal, F. Browne, G. Gey, H. S. Jung, J. Taprogge, Zs. Vajta, J. Wu, A. Yagi, H. Baba, G. Benzoni, K. Y. Chae, F. C. L. Crespi, N. Fukuda, R. Gernhäuser, N. Inabe *et al.*, *Phys. Rev. Lett.* **111**, 152501 (2013).
- [22] S. Ilieva, M. Thürauf, Th. Kröll, R. Krücken, T. Behrens, V. Bildstein, A. Blazhev, S. Bönig, P. A. Butler, J. Cederäll, T. Davinson, P. Delahaye, J. Diriken, A. Ekström, F. Finke, L. M. Fraile, S. Franchoo, Ch. Fransen, G. Georgiev, R. Gernhäuser, D. Habs *et al.*, *Phys. Rev. C* **89**, 014313 (2014).
- [23] C. X. Yuan, Z. Liu, F. R. Xu, P. M. Walker, Z. Podolyák, C. Xu, Z. Z. Ren, B. Ding, M. L. Liu, X. Y. Liu, H. S. Xu, Y. H. Zhang, X. H. Zhou, and W. Zuo, *Phys. Lett. B* **762**, 237 (2016).
- [24] J. Q. Chen, *Nucl. Phys. A* **626**, 686 (1997).
- [25] Y. M. Zhao, N. Yoshinaga, S. Yamaji, J. Q. Chen, and A. Arima, *Phys. Rev. C* **62**, 014304 (2000).
- [26] J. Q. Chen, B. Q. Chen, and A. Klein, *Nucl. Phys. A* **554**, 61 (1993); J. Q. Chen, *ibid.* **562**, 218 (1993).
- [27] Y. A. Luo and J. Q. Chen, *Phys. Rev. C* **58**, 589 (1998).
- [28] Y. M. Zhao, S. Yamaji, N. Yoshinaga, and A. Arima, *Phys. Rev. C* **62**, 014315 (2000).
- [29] Y. M. Zhao, N. Yoshinaga, S. Yamaji, and A. Arima, *Phys. Rev. C* **62**, 014316 (2000).
- [30] L. Y. Jia, H. Zhang, and Y. M. Zhao, *Phys. Rev. C* **75**, 034307 (2007); **76**, 054305 (2007).
- [31] Y. Lei, Z. Y. Xu, Y. M. Zhao, and A. Arima, *Phys. Rev. C* **82**, 034303 (2010); Y. Lei, Y. M. Zhao, and A. Arima, *ibid.* **84**, 044301 (2011).
- [32] Y. Lei, H. Jiang, and S. Pittel, *Phys. Rev. C* **102**, 024310 (2020).
- [33] M. A. Caprio, F. Q. Luo, K. Cai, V. Hellemans, and Ch. Constantinou, *Phys. Rev. C* **85**, 034324 (2012); M. A. Caprio, F. Q. Luo, K. Cai, Ch. Constantinou, and V. Hellemans, *J. Phys. G: Nucl. Part. Phys.* **39**, 105108 (2012).
- [34] H. Jiang, Y. Lei, G. J. Fu, Y. M. Zhao, and A. Arima, *Phys. Rev. C* **86**, 054304 (2012); H. Jiang, Y. Lei, C. Qi, R. Liotta, R. Wyss, and Y. M. Zhao, *ibid.* **89**, 014320 (2014).
- [35] Y. Y. Cheng, Y. M. Zhao, and A. Arima, *Phys. Rev. C* **94**, 024307 (2016); Y. Y. Cheng, C. Qi, Y. M. Zhao, and A. Arima, *ibid.* **94**, 024321 (2016).
- [36] Y. Y. Cheng, H. Wang, J. J. Shen, X. R. Zhou, Y. M. Zhao, and A. Arima, *Phys. Rev. C* **100**, 024321 (2019).
- [37] G. J. Fu and C. W. Johnson, *Phys. Lett. B* **809**, 135705 (2020).
- [38] G. J. Fu, C. W. Johnson, P. Van Isacker, and Z. Z. Ren, *Phys. Rev. C* **103**, L021302 (2021).
- [39] Y. Y. Cheng, J. J. Shen, G. J. Fu, X. R. Zhou, Y. M. Zhao, and A. Arima, *Phys. Rev. C* **100**, 014318 (2019).
- [40] G. J. Fu, Y. Lei, Y. M. Zhao, S. Pittel, and A. Arima, *Phys. Rev. C* **87**, 044310 (2013).
- [41] Y. Y. Cheng, Y. M. Zhao, and A. Arima, *Phys. Rev. C* **97**, 024303 (2018).
- [42] B. C. He, L. Li, Y. A. Luo, Y. Zhang, F. Pan, and J. P. Draayer, *Phys. Rev. C* **102**, 024304 (2020).
- [43] Y. Lei, Y. Lu, and Y. M. Zhao, *Chin. Phys. C* **45**, 054103 (2021).
- [44] Y. M. Zhao and A. Arima, *Phys. Rep.* **545**, 1 (2014).
- [45] R. Machleidt, *Phys. Rev. C* **63**, 024001 (2001).
- [46] M. Hjorth-Jensen, T. T. S. Kuo, and E. Osnes, *Phys. Rep.* **261**, 125 (1995).
- [47] T. Otsuka, T. Suzuki, M. Honma, Y. Utsuno, N. Tsunoda, K. Tsukiyama, and M. Hjorth-Jensen, *Phys. Rev. Lett.* **104**, 012501 (2010).
- [48] G. Bertsch, J. Borysowicz, H. McManus, and W. G. Love, *Nucl. Phys. A* **284**, 399 (1977).
- [49] H. Wang, N. Aoi, S. Takeuchi, M. Matsushita, T. Motobayashi, D. Steppenbeck, K. Yoneda, H. Baba, Zs. Dombrádi, K. Kobayashi, Y. Kondo, J. Lee, H. Liu, R. Minakata, D. Nishimura, H. Otsu, H. Sakurai, D. Sohler, Y. Sun, Z. Tian *et al.*, *Phys. Rev. C* **94**, 051301(R) (2016).
- [50] P. Ring and P. Schuck, *The Nuclear Many-Body Problem*, (Springer-Verlag, New York, 1980), and references therein.
- [51] D. J. Rowe, *Nuclear Collective Motion: Models and Theory*, (World Scientific Publishing, Singapore, 2010), and references therein.
- [52] R. L. Hatch and S. Levit, *Phys. Rev. C* **25**, 614 (1982).
- [53] A. Bohr and B. R. Mottelson, *Phys. Scr.* **25**, 28 (1982).
- [54] A. Leviatan, *Ann. Phys.* **179**, 201 (1987).
- [55] M. A. Caprio, *J. Phys. A: Math. Gen.* **38**, 6385 (2005).
- [56] Y. K. Gambhir, A. Rimini, and T. Weber, *Phys. Rev.* **188**, 1573 (1969).
- [57] R. D. Lawson, *Theory of the Nuclear Shell Model* (Clarendon Press, Oxford, 1980).
- [58] I. Talmi, *Simple Models of Complex Nuclei: The Shell Model and Interacting Boson Model* (Harwood Academic Publishers, Switzerland, 1993).
- [59] <http://www.nndc.bnl.gov/ensdf/>.
- [60] J. Taprogge, A. Jungclaus, H. Grawe, S. Nishimura, P. Doornenbal, G. Lorusso, G. S. Simpson, P. A. Söderström, T. Sumikama, Z. Y. Xu, H. Baba, F. Browne, N. Fukuda, R. Gernhäuser, G. Gey, N. Inabe, T. Isobe, H. S. Jung, D. Kameda, G. D. Kim *et al.*, *Phys. Rev. Lett.* **112**, 132501 (2014).
- [61] N. Hoteling, W. B. Walters, B. E. Tomlin, P. F. Mantica, J. Pereira, A. Becerril, T. Fleckenstein, A. A. Hecht, G. Lorusso, M. Quinn, J. S. Pinter, and J. B. Stoker, *Phys. Rev. C* **76**, 044324 (2007).
- [62] Y. X. Luo, J. O. Rasmussen, C. S. Nelson, J. H. Hamilton, A. V. Ramayya, J. K. Hwang, S. H. Liu, C. Goodin, N. J. Stone, S. J. Zhu, N. T. Brewer, K. Li, I. Y. Lee, G. M. Ter-Akopian, A. V. Daniel, M. A. Stoyer, R. Donangelo, W. C. Ma, and J. D. Cole, *Nucl. Phys. A* **874**, 32 (2012).
- [63] J. C. Batchelder, N. T. Brewer, C. J. Gross, R. Grzywacz, J. H. Hamilton, M. Karny, A. Fijalkowska, S. H. Liu, K. Miernik, S. W. Padgett, S. V. Paulaskas, K. P. Rykaczewski, A. V. Ramayya, D. W. Stracener, and M. Wolinska-Cichocka, *Phys. Rev. C* **89**, 054321 (2014).
- [64] G. S. Simpson, G. Gey, A. Jungclaus, J. Taprogge, S. Nishimura, K. Sieja, P. Doornenbal, G. Lorusso, P.-A. Söderström, T. Sumikama, Z. Y. Xu, H. Baba, F. Browne, N. Fukuda, N. Inabe, T. Isobe, H. S. Jung, D. Kameda, G. D. Kim, Y.-K. Kim *et al.*, *Phys. Rev. Lett.* **113**, 132502 (2014).
- [65] I. O. Morales, P. Van Isacker, and I. Talmi, *Phys. Lett. B* **703**, 606 (2011).
- [66] T. Bäck, C. Qi, B. Cederwall, R. Liotta, F. Ghazi Moradi, A. Johnson, R. Wyss, and R. Wadsworth, *Phys. Rev. C* **87**, 031306(R) (2013).
- [67] C. Qi, *Phys. Rev. C* **94**, 034310 (2016).